Differences in Fatty Acid Metabolic Disorder Between Ischemic Myocardium and Doxorubicin-Induced Myocardial Damage: Assessment Using BMIPP Dynamic SPECT with Analysis by the Rutland Method

Kakuya Kitagawa, MD[1]; Kan Takeda, MD[2]; Kimimasa Saito, MD[3]; Shinya Okamoto, MD[4]; Katsutoshi Makino, MD[4]; Hisato Maeda, PhD[5]; and Takashi Ichihara, PhD[6]

[1]Department of Radiology, Matsusaka Central Hospital, Mie, Japan; [2]Department of Radiology, Mie University, Mie, Japan; [3]Department of Internal Medicine, Yamamoto General Hospital, Mie, Japan; [4]Department of Internal Medicine, Matsusaka Central Hospital, Mie, Japan; [5]Fujita Health University, Aichi, Japan; and [6]Toshiba Corporation, Tokyo, Japan

Dynamic myocardial SPECT data acquired with 15-^{123}I-(*p*-iodophenyl)-3-(*R,S*)-methylpentadecanoic acid (BMIPP) were analyzed by the Rutland method. The relative time–activity curves generated from dynamic SPECT in normal control subjects were compared with similar curves from patients with established ischemic heart disease (IHD) and doxorubicin-induced myocardial damage (DxMD). Comparison of such time–activity curves may provide some indirect information concerning qualitative differences in BMIPP metabolism. **Methods:** Thirteen patients with various malignancies who received doxorubicin, 16 patients with IHD, and 15 normal control subjects were examined. Immediately after the bolus injection of BMIPP, dynamic data acquisition with a 3-head SPECT system was started and continued for 15 min. Using the time–activity curves of the myocardium as the output function (Mo(t)) and the time–activity curves of the left ventricular cavity as the input function (B(t)), the Rutland equation was calculated: $Mo(t)/B(t) = F + K \int B(t)dt/B(t)$, where F is the blood − background subtraction factor and K is the uptake constant. The duration of the linear portion in this equation and the K values were evaluated. **Results:** Mo(t)/B(t) was plotted against $\int B(t)dt/B(t)$. Mo(t)/B(t) showed a good linear correlation with $\int B(t)dt/B(t)$ from 30 s to 230 ± 57 s in normal control subjects. The duration of this linearity was prolonged to 317 ± 79 s in DxMD ($P = 0.0014$) and shortened to 182 ± 58 s in IHD ($P = 0.039$). The mean K value was 0.0740 ± 0.0184 in normal control subjects, significantly higher than the K values of 0.0599 ± 0.0148 in DxMD patients ($P = 0.026$) and 0.0497 ± 0.0189 ($P = 0.0020$) in IHD patients. **Conclusion:** Analysis of BMIPP dynamic SPECT data by the Rutland method is useful for detecting qualitative differences in BMIPP metabolism in various types of myocardial damage. It is speculated that the fatty acid metabolic disorder is characterized by a delay in metabolism in DxMD and by increased backdiffusion in IHD.

Key Words: BMIPP; dynamic SPECT; ischemic heart disease; doxorubicin-induced myocardial damage; Rutland analysis

J Nucl Med 2002; 43:1286–1294

Fatty acids are known to play a major role as cardiac energy sources under normal aerobic conditions (*1*). 15-^{123}I-(*p*-Iodophenyl)-3-(*R,S*)-methylpentadecanoic acid (BMIPP) is a radioiodinated fatty acid analog with a methyl branch at the β3 position. The structure of BMIPP inhibits its rapid catabolism in the myocardium; thus, BMIPP has a long retention time in the myocardium due to incorporation into the triglyceride pool, which is a useful characteristic in clinical SPECT imaging (*2,3*).

There is increasing interest in the mechanism of BMIPP washout rather than uptake because several studies have reported that BMIPP possesses the unique property of perfusion–metabolism mismatch—that is, a decrease in BMIPP uptake with relatively preserved myocardial perfusion on SPECT images in patients with ischemic heart disease (IHD) (*4,5*). Recent studies using an animal model provided some evidence that backdiffusion of BMIPP from the myocardium is increased significantly in the early phase under ischemic conditions. However, little is known about the early kinetics of BMIPP in humans (*6,7*).

Our previous study demonstrated the clinical feasibility of dynamic SPECT with BMIPP for the early detection of doxorubicin-induced cardiomyopathy (*8*). In that study, the quantitative evaluation of fatty acid metabolism using the Rutland method was shown to be very useful for analyzing the early kinetics of injected BMIPP. Thus, this study was

Received Dec. 28, 2001; revision accepted Jun. 4, 2002.

For correspondence or reprints contact: Kakuya Kitagawa, MD, Department of Radiology, Matsusaka Central Hospital, 102 Kobo Kawaimachi, Matsusaka, Mie 515-8566, Japan.

E-mail: kakuya@clin.medic.mie-u.ac.jp

TABLE 1
Patients with DxMD

Patient	Age (y)	Sex	Malignant disease	Total administered dose of doxorubicin (mg/m^2)	Time between final administration and dynamic SPECT (d)
1*	42	F	Breast cancer	360	0
2	78	M	Non-Hodgkin's lymphoma	125	2
3*	78	M	Non-Hodgkin's lymphoma	30	7
4	59	M	Small cell lung cancer	255	9
5	67	F	Non-Hodgkin's lymphoma	145	10
6	79	F	Non-Hodgkin's lymphoma	110	10
7	41	F	Acute myelocytic leukemia	100	11
8*	45	M	Malignant mesothelioma	240	12
9*	79	F	Non-Hodgkin's lymphoma	75	13
10	68	F	Non-Hodgkin's lymphoma	90	16
11	65	M	Small cell lung cancer	75	16
12	49	F	MALT of stomach	400	16
13	68	M	Non-Hodgkin's lymphoma	150	19
14	49	M	Hepatoma	85	22
15	37	M	Non-Hodgkin's lymphoma	180	23
16	79	M	Non-Hodgkin's lymphoma	220	29

*Dynamic SPECT was performed both before and after chemotherapy.
MALT = mucosa-associated lymphoid tissue.

undertaken to further assess the usefulness of the Rutland method for evaluating abnormalities in myocardial fatty acid metabolism and to compare the differences in the early kinetics of BMIPP among subjects with normal myocardium, ischemic myocardium, and doxorubicin-induced myocardial damage (DxMD).

MATERIALS AND METHODS

DxMD

Sixteen patients (9 men, 7 women; mean age, 60.7 y) with malignancies (9 patients with malignant lymphoma, 2 with lung cancer, 1 with leukemia, 1 with breast cancer, 1 with hepatocellular carcinoma, 1 with mucosa-associated lymphoid tissue of the stomach, and 1 with malignant mesothelioma) received doxorubicin. The total administered dose of doxorubicin in the 16 patients ranged from 30 to 400 mg/m^2, as shown in Table 1. Dynamic myocardial SPECT with BMIPP was performed after the final administration.

IHD

Thirteen patients (5 men, 8 women; mean age, 67.2 y) with areas showing apparent redistribution on ^{201}Tl myocardial SPECT were considered to have ischemic myocardium (Table 2). In 11 of the 13 patients, coronary angiography demonstrated significant stenosis in the segments of the coronary arteries corresponding to the areas of redistribution seen on ^{201}Tl myocardial SPECT. Redistribution in the 2 patients with nonstenotic coronary arteries was considered to be due to diabetic microangiopathy and syndrome X.

Normal Control Subjects

Ten patients with malignancy before chemotherapy and 5 patients with suspected episodes of IHD were classified as normal control subjects. The patients with malignancy had no history of diabetes or chest pain and showed no abnormalities on electrocardiography at rest or on echocardiography. In addition, the patients with suspected episodes of IHD did not show any abnormalities on electrocardiography, echocardiography, or ^{201}Tl myocardial SPECT. Thus, the total number of normal control subjects was 15 (8 men, 7 women; mean age, 67.4 y).

Radiopharmaceuticals

The ^{123}I-labeled BMIPP used was a commercially available product (Nihon Medi-Physics Co., Ltd., Hyogo, Japan). The formulation contained 111 MBq (3 mCi) BMIPP (0.6 mg) dissolved in an aqueous solution (1 mL) of ursodeoxycholic acid (10.5 mg).

TABLE 2
Patients with IHD

Patient	Age (y)	Sex	Ischemic segment on myocardial SPECT with ^{201}Tl	Coronary arteriographic finding
1	76	F	Anterior wall	LAD 99%
2	65	F	Inferior wall	RCA 75%
3	70	F	Inferior wall	RCA 90%
4	67	M	Lateral wall	CX 75%
5	67	F	Lateral wall	CX 75%
6	78	M	Anteroseptum	LAD 90%
7	75	F	Anteroseptum	LAD 99%
8	57	M	Anteroseptum	LAD 75%
9	69	F	Anteroseptum	LAD 25%*
10	54	F	Anteroseptum	Normal†
11	63	M	Lateral wall	CX 99%
12	64	F	Anteroseptum	LAD 90%
13	50	M	Anterior wall	LAD 99%

*Diabetic microangiopathy.
†Syndrome X.
LAD = left anterior descending artery; RCA = right coronary artery; CX = left circumflex artery.

The radiochemical purity was >98%. The product showed a single, homogeneous radioactive component on thin-layer chromatographic analysis.

Instrumentation

Dynamic myocardial SPECT imaging was performed using a 3-head SPECT system (GCA-9300A; Toshiba, Tokyo, Japan) equipped with a high-resolution, parallel-hole collimator.

Imaging Protocol and Data Acquisition

After breakfast on the day of examination, all subjects were instructed to take nothing by mouth until completion of the study. Two hours after breakfast, 111 MBq BMIPP were injected through an antecubital vein. Immediately after bolus injection, dynamic myocardial SPECT imaging was performed every 30 s. Dynamic data were acquired with continuous rotation. Camera rotation of 120° around the chest in 30 s provided 360° projection coverage. Thirty series of projection data (30-s data) were acquired within a period of 15 min. Static myocardial SPECT imaging was performed 30 min after injection (early images) and was repeated 3 h later (delayed images).

Ninety projection images were acquired over 360° in 4° increments with a 64 × 64 matrix in both dynamic and static myocardial SPECT studies. Projection data were collected from a main window (159 keV ± 12%) and two 3% scatter-rejection windows. Scatter correction for each pixel was performed using the triple-energy window method (*9*). Reconstruction of transaxial tomographic images was performed with a 64 × 64 matrix for dynamic SPECT images and with a 128 × 128 matrix for static SPECT images using Butterworth and ramp filters. The slice thickness of each tomographic image was 12.8 mm.

Analysis of Dynamic SPECT Data by Rutland Method

A region of interest (ROI) was placed over the entire myocardium in a short-axial midventricular slice in normal control subjects and patients with DxMD, whereas the ROI was placed on the ischemic segment in patients with IHD. The mean counts per pixel were calculated, and the time–activity curve was obtained from 30 s to 15 min. Using the time–activity curve of myocardium (Mo(t)) as the output function and the time–activity curve of the left ventricular cavity (B(t)) as the input function, the Rutland equation is defined as follows (*10*):

$$Mo(t)/B(t) = F + K \int B(t)dt/B(t),$$

where K is the uptake constant and F is the blood − background subtraction factor (Fig. 1A).

Mo(t)/B(t) and ∫B(t)dt/B(t) for each t (i.e., for each scan time) were calculated from the dynamic SPECT data. Mo(t)/B(t) was plotted against ∫B(t)dt/B(t) to test for a linear correlation between the 2 variables. The presence of a linear portion indicated that there was no significant excretion of BMIPP from the myocardium during that period.

Analysis of Static SPECT Images

The early and delayed myocardial SPECT images obtained with BMIPP were visually assessed on long-axis and short-axis left ventricular slices. BMIPP uptake in each segment was scored on

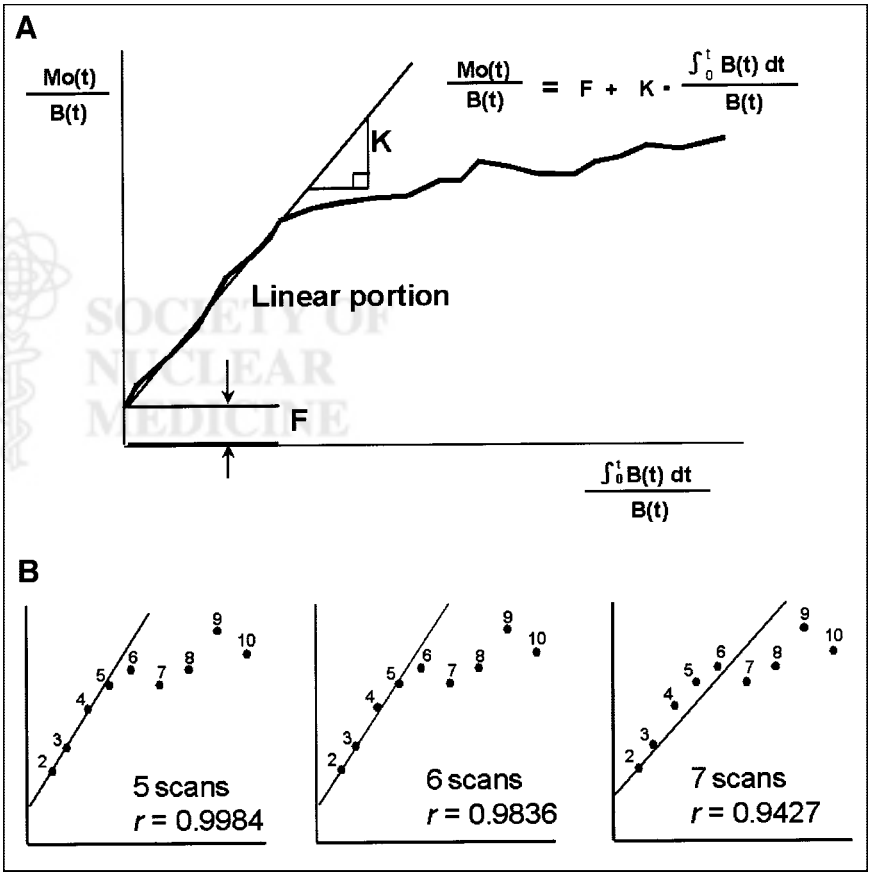

FIGURE 1. (A) Diagram of Rutland equation. Mo(t)/B(t) and ∫B(t)dt/B(t) for each scan time (t) can be calculated from dynamic SPECT data. By plotting Mo(t)/B(t) against ∫B(t)dt/B(t), the linear portion can be identified on curve. Presence of linear portion indicates that there is no significant excretion of BMIPP from myocardium during this period. (B) Determination of duration of linear portion in Rutland equation. Linear correlation coefficients from start of second scan (30 s) to specific scans were calculated and compared. For example, linear correlation coefficient (*r*) values are 0.9984 and 0.9836 up to 5 and 6 scans, respectively, in this case. Both values are considered to be sufficiently high to indicate a straight line. However, correlation coefficient up to 7 scans rapidly falls to 0.9427. Thus, we determined duration of linear portion to be up to 6 scans in this case. Slope (K value) can then be calculated.

the basis of the consensus of 2 experienced observers who were unaware of the results of dynamic SPECT and the patients' backgrounds using a 3-point grading system (2 = normal, 1 = reduced, 0 = absent). Disagreements between the observers were resolved by consensus.

Assessments

We attempted to determine the duration and the slope (uptake constant = K value) of the linear portion to compare the results among normal control subjects, DxMD patients, and IHD patients. To determine the duration of the linear portion, the linear correlation coefficients from the second scan to specific scans were calculated in each patient. The data from the first scan were omitted because they showed a high degree of variability due to the tremendously high input counts associated with bolus injection. A linear correlation coefficient of >0.98 was considered to correspond to a straight line and, therefore, was used as an index to determine the duration of the linear portion in the Rutland equation (Fig. 1B). When the duration of the linear portion is determined, the slope (K value) can be calculated.

Statistical Analysis

All data are presented as mean ± SD. Differences in the duration of the linear portion in the Rutland equation and differences in K values between normal control subjects and DxMD patients and between normal control subjects and IHD patients were assessed by the Student t test. Differences with $P < 0.05$ were considered statistically significant.

RESULTS

Duration of Linear Portion in Rutland Equation

The serial changes in the linear correlation coefficient during the period from the second scan up to each scan in normal control subjects, DxMD patients, and IHD patients are shown in Figures 2A–2C. A linear correlation coefficient of >0.98 was used as an index of linearity in the Rutland equation. The duration of linear correlation was 230 ± 57 s in normal control subjects and was significantly prolonged in DxMD patients (317 ± 79 s; $P = 0.0014$) and significantly shortened in IHD patients (182 ± 58 s; $P = 0.039$). These findings suggest that there is no significant excretion of BMIPP from the myocardium during the period from 30 s to ~230 s in normal control subjects, from 30 s to ~317 s in DxMD patients, and from 30 s to ~182 s in IHD patients (Fig. 3A).

K Values

K values (uptake constants) were calculated as the slope of the linear portion in the Rutland equation. The mean K value was 0.0740 ± 0.0184 in normal control subjects, significantly higher than that in DxMD patients (0.0599 ± 0.0148; $P = 0.026$) and in IHD patients (0.0497 ± 0.0189; $P = 0.0020$) (Fig. 3B).

Static Myocardial SPECT Images

Among normal control subjects, none showed reduced or absent uptake of BMIPP on static SPECT images. Among DxMD patients, only 1 showed reduced uptake in the anterolateral wall. Among IHD patients, 6 showed reduced

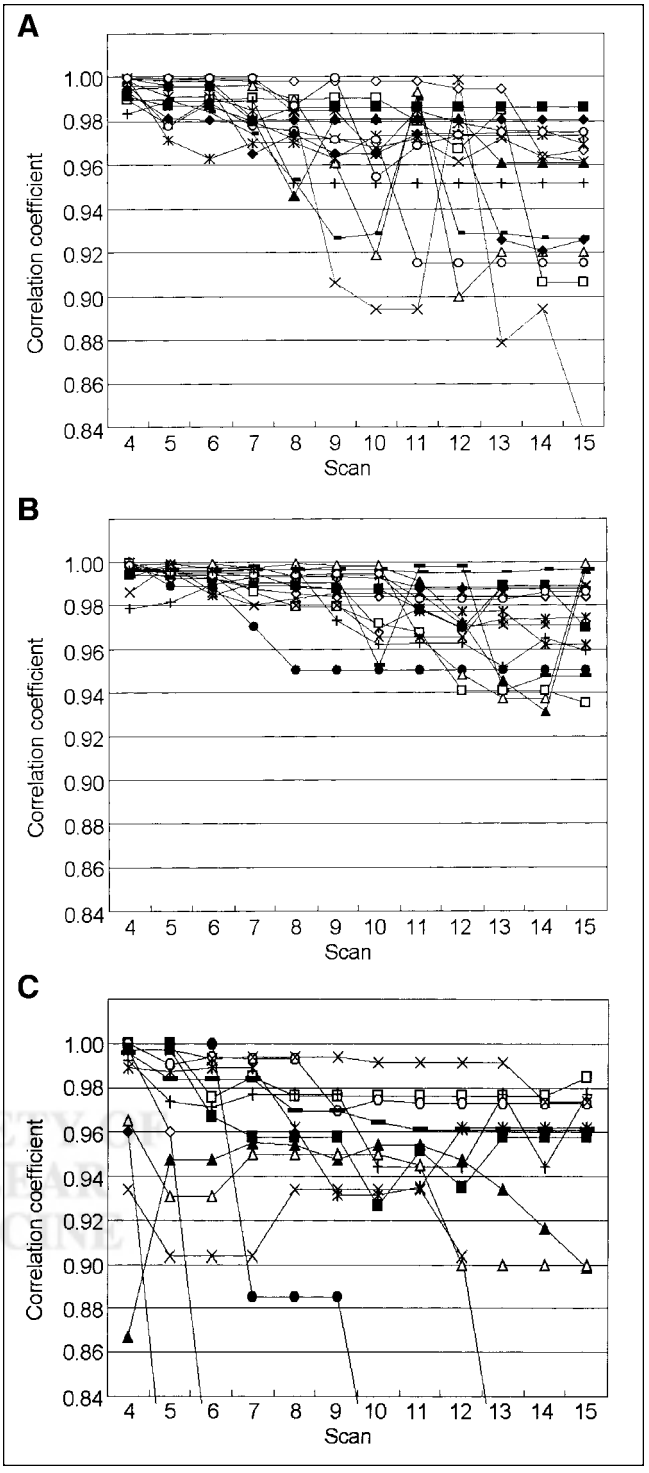

FIGURE 2. Serial changes in linear correlation coefficients from second scan to specific scans in normal control subjects (A), patients with DxMD (B), and patients with IHD (C). High linear correlation coefficients are maintained up to ~7 scans in normal control subjects, and duration of linear portion is prolonged in DxMD patients and shortened in IHD patients. Individual symbols (○, ◇, △, and so forth) represent different patients.

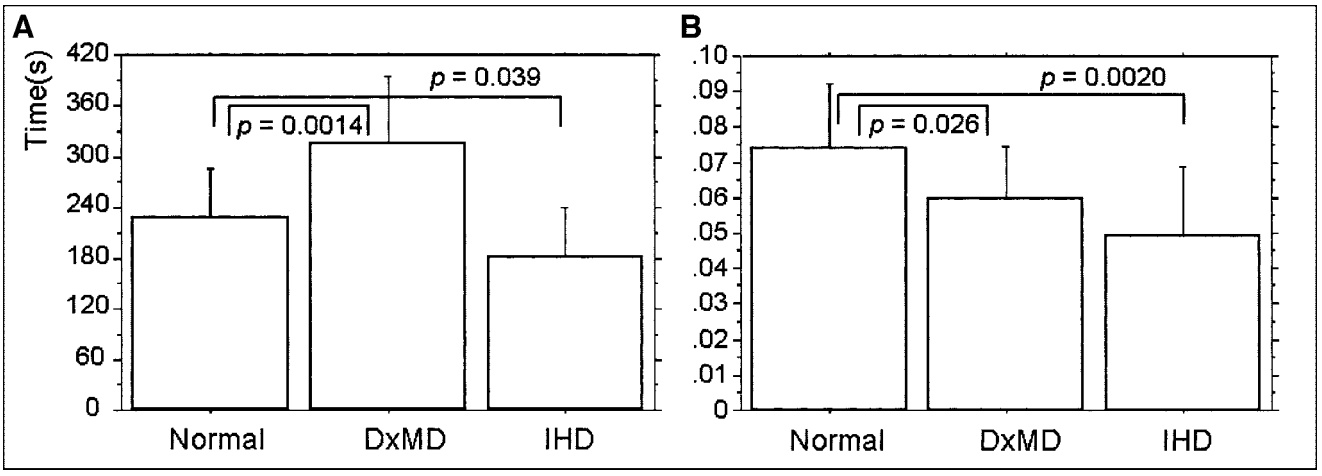

FIGURE 3. Comparison of duration of linear portion (A) and K value (B). Duration of linear portion is significantly prolonged in DxMD and shortened in IHD. K value is significantly decreased in both DxMD and IHD.

uptake of BMIPP in the ischemic segment, whereas the other 7 patients showed no BMIPP uptake abnormalities in the ischemic segment. No relationship was found between shortening of the duration of the linear portion in the Rutland equation and reduced BMIPP uptake on static images.

Representative Cases

Case 1. A 65-y-old man with small cell carcinoma of the lung. The total amount of doxorubicin administered was 75 mg/m^2. The patient had no history of IHD and was examined by BMIPP SPECT 10 d after the final dose of chemotherapy. No regional abnormalities in BMIPP uptake were observed on static SPECT images either before or after chemotherapy (Figs. 4A and 4B). On dynamic study, the linear portion in the Rutland equation was prolonged after chemotherapy compared with that before chemotherapy (Figs. 4C and 4D). Mo(t)/B(t) showed a good linear correlation with $\int B(t)dt/B(t)$ during the period up to 210 s, which was substantially prolonged. The K value decreased from 0.0921 to 0.0658 after chemotherapy.

Case 2. A 76-y-old woman with a history of hypertension, hyperlipidemia, and chest pain. ^{201}Tl SPECT demonstrated ischemic myocardium in the anteroseptal left ventricular wall. Static BMIPP SPECT images showed no abnormalities in the ischemic segment (Fig. 5A). However, the duration of the linear portion in the Rutland equation was substantially shortened (120 s) in the ischemic segment. The K value was 0.0335 in the ischemic segment (Fig. 5B).

DISCUSSION

The mechanism of BMIPP uptake and retention is considered to be as follows (Fig. 6). Once BMIPP passes from the blood into the myocardial cells through a transporter or passive diffusion, BMIPP is acylated in the presence of adenosine triphosphate (ATP) and coenzyme A (CoA) and transformed to BMIPP-CoA (*11,12*). The BMIPP-CoA produced is hydrophilic, thus facilitating its intracellular retention. BMIPP-CoA is not initially metabolized by β-oxidation, because the methyl group precludes the formation of the keto-acyl CoA intermediate, but is esterified to triglycerides and stored in the lipid pool in the cytosol for a prolonged period (*2,3*). A part of the BMIPP-CoA is degraded by initial α-oxidation, which occurs mainly in the peroxisomes, producing α-methyl-*p*-iodophenyltetradecanoic acid (AMIPT). Then, AMIPT is metabolized by subsequent cycles of β-oxidation in the mitochondria, with *p*-iodophenylacetic acid (PIPA) formed as the final metabolite. During the β-oxidation process, several intermediate metabolites, including *p*-iodophenyldodecanoic acid ($PIPC_{12}$), *p*-iodophenylhexanoic acid ($PIPC_6$), and so forth, are also produced (*13–16*). These intermediate and final metabolites of BMIPP do not accumulate intracellularly and leave the cell immediately after formation (*11*). This characteristic metabolic pathway of BMIPP may explain the small amount of washout observed in the normal myocardium at rest, but washout can be increased by exercise (*17*).

Although dynamic SPECT study permits precise analysis of the early and rapid kinetics of radiotracers, it should be emphasized that there is significant contamination by background activity. This is the reason that the myocardial dynamic curves for BMIPP, as reported by Matsunari et al. (*18*) and by our group (*19*), showed higher (or sometimes the highest) counts in the early (blood flow) phase than that in the late phase after the accumulation of BMIPP in the myocardial cells. Kobayashi et al. (*20*) reported that the distribution of BMIPP possibly reflected myocardial perfusion in the early phase (2–5 min) after the bolus injection of BMIPP. The Rutland method is theoretically effective for subtracting the vascular background activity in intramural and epicardial coronary arteries in the early phase and permits accurate analysis of early BMIPP kinetics in the myocardium. However, interstitial background activity cannot be subtracted effectively using this method. Therefore, Rutland analysis is rarely applied to severely damaged myocardium with abundant interstitial tissue.

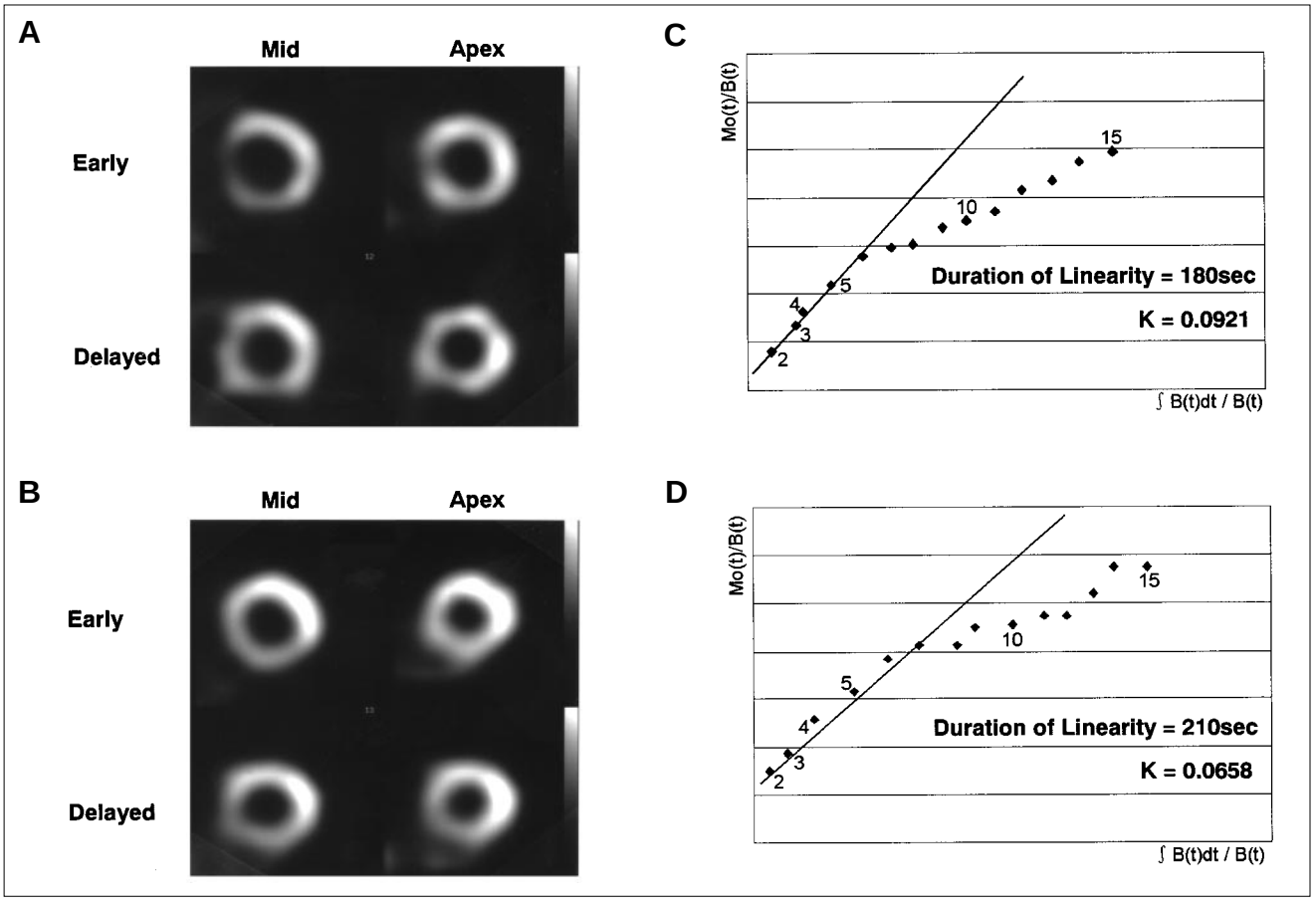

FIGURE 4. Early and delayed static BMIPP images from patient with DxMD before (A) and after (B) chemotherapy. No regional uptake abnormality is seen on static images. Rutland analysis of dynamic BMIPP SPECT after chemotherapy (D) demonstrates prolonged linear portion and decreased K value compared with that before chemotherapy (C).

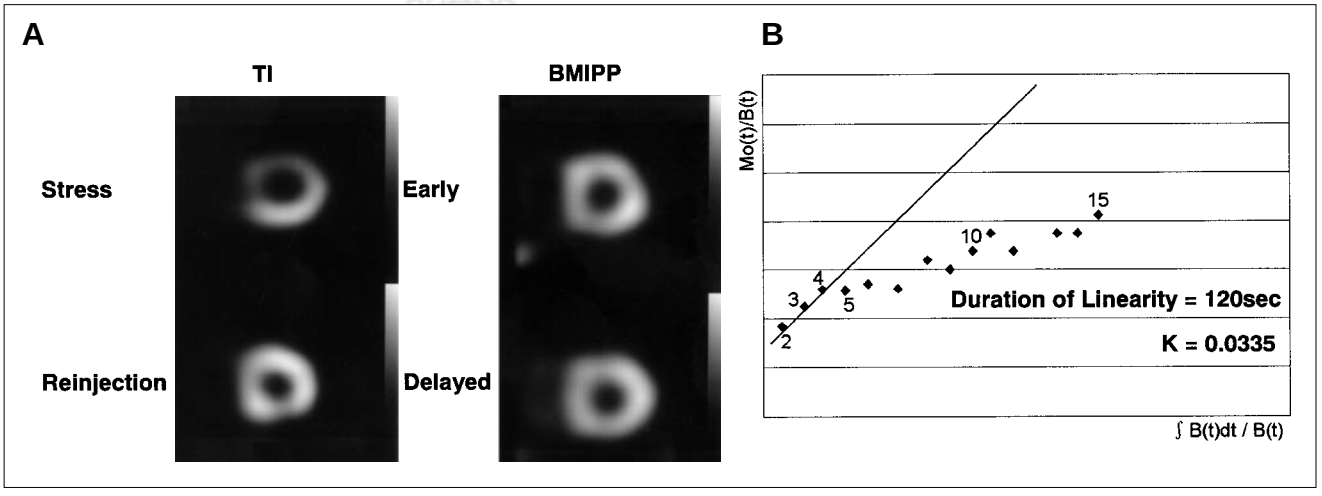

FIGURE 5. (A) Stress and rest ^{201}Tl and static BMIPP images of patient with angina pectoris. Coronary angiography shows significant coronary artery stenosis in left anterior descending artery. Redistribution is observed in anterior segment on ^{201}Tl images, whereas static BMIPP images show no uptake abnormality in this segment. (B) Rutland analysis of dynamic BMIPP SPECT demonstrates shortened duration of linear correlation with decreased K value.

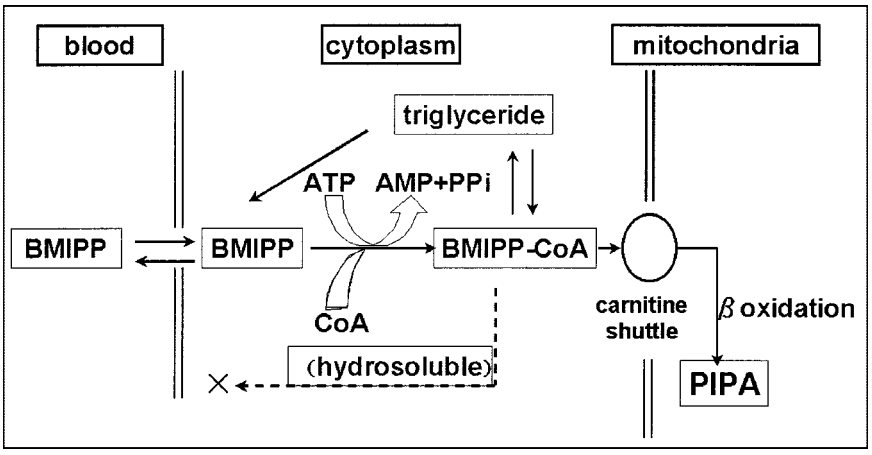

FIGURE 6. Schematic diagram of metabolic pathway of BMIPP. ATP = adenosine triphosphate; AMP = adenosine monophosphate; PPi = pyrophosphate; CoA = coenzyme A; PIPA = *p*-iodophenylacetic acid.

Mo(t)/B(t) showed a good linear correlation with $\int B(t)dt/B(t)$ during the period from 30 s to 230 ± 57 s in normal control subjects. This finding indicates that BMIPP accumulates in the myocardium at a constant rate (K) without any excretion during this period. According to several experimental studies, the excretion of the intermediate and final metabolites (AMIPT, isopentadecanoic acid, PIPA, and so forth) into the blood from the normal myocardium begins ~2 min after injection and shows a gradual increase, with peak excretion at 5–10 min (*5,14,21*). We believe that these experimental findings agree with our clinical results, although there are slight differences in the measured times because of the different calculation methods used. Thus, we speculate that the duration of the linear portion in the Rutland equation depends on the excretion of the BMIPP metabolites in normal subjects.

The linear portion in the Rutland equation was maintained for a longer period and K values were decreased in DxMD patients compared with that of normal subjects, although static SPECT images showed no abnormalities in most cases (15/16 cases). Neither the precise mechanism of DxMD nor the fatty acid metabolism in DxMD has been elucidated yet. However, some researchers have suggested that, from the histopathologic point of view, mitochondrial damage may precede the myocardial damage induced by doxorubicin administration (*22–25*). Seraydarian and Artaza (*26*) and Neri et al. (*27*) have pointed out that ATP concentrations inside myocardial cells decrease because of the impaired mitochondrial respiratory function caused by doxorubicin cardiotoxicity. Thus, mitochondrial damage may well lead to delayed fatty acid metabolism, and subsequent ATP depletion seems to slow the conversion of BMIPP to BMIPP-CoA (*7*). With regard to the Rutland equation, the longer linear portion may reflect the delay in fatty acid metabolism corresponding to a lack of excretion of final and intermediate metabolites over a longer period, and the decrease in the K value may reflect the slow conversion of BMIPP to BMIPP-CoA.

It has been shown in animal models that the early kinetics of BMIPP in ischemic myocardium is characterized by increased backdiffusion of nonmetabolized BMIPP and decreased excretion of intermediate and final metabolites due to a fall in ATP concentration (*5,16,21,28*). Most backdiffusion occurs within 1 min after BMIPP injection. In our study, the duration of the linear portion in the Rutland equation was shorter in IHD patients. Generally speaking, ischemic myocardium suffers from varying degrees of tissue damage. Severely damaged myocardium might show a large amount of backdiffusion of nonmetabolized BMIPP, resulting in poor (or even absent) linearity in the Rutland equation. On the other hand, mildly damaged myocardium might show a relatively small amount of backdiffusion, resulting in fairly well preserved linearity, with only a decreased uptake constant. Furthermore, ischemic myocardium is not a homogeneous tissue from either the pathophysiologic or the metabolic point of view. Rather, it can be considered as a mixture of myocardial tissues suffering from damage of varying degrees of severity. Because the dynamic data obtained by SPECT show the average of such heterogeneity, the shortening of the period of linearity in the ischemic myocardium depends on the proportions of the constituent tissues in the damaged myocardium. If the ischemic myocardium consists mainly of severely injured tissue, the duration of the linear portion will be shortened to 1 or 2 min and the K value will show a significant decrease. Otherwise, the period of linearity will be longer and the K value will be larger. These are the reasons that the duration of the linear portion varied so widely from 1 min to several minutes in IHD patients, as shown in Figure 3C. The value of 3 min—that is, the average duration of the linear portion in ischemic myocardium obtained in this study—was just an incidental value calculated in our series of patients. What is important is the fact that the duration of the linear portion is shortened by varying degrees in ischemic myocardium. Linearity is poor in extensively damaged myocardium because of the increased interstitial tissue and intensified backdiffusion. Conversely, poor linearity reflects the severity of myocardial damage.

A comparison of the Rutland equations in DxMD and IHD is presented in Figure 7. The duration of the linear

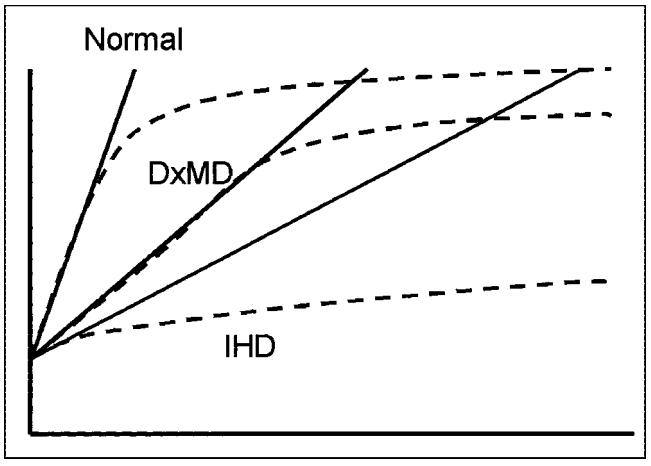

FIGURE 7. Comparison of typical curves (dashed lines) in Rutland equation among subjects with normal myocardium, DxMD, and IHD. Solid lines indicate linear portion of corresponding curves.

portion in the Rutland equation is prolonged in DxMD subjects and shortened in IHD subjects. The K value is decreased in both DxMD and IHD. We speculate that these characteristics of the Rutland equation reflect the features of the fatty acid metabolic disorders in DxMD and IHD (i.e., delayed metabolism in DxMD and increased backdiffusion in IHD).

Several limitations of our study should be acknowledged. The Rutland method is theoretically effective for subtracting the activities in the reversible compartment. However, it is valid only when myocardial and arterial blood activity is measured directly. In SPECT studies, quantitative measurements are blurred by the ROI setting, myocardial movement, scatter, attenuation, and count recovery loss due to the low full width at half maximum. It is true that attenuation correction, as well as scatter correction, is necessary to ensure accuracy in quantitative SPECT analysis. However, in this study only scatter correction was performed. Attenuation correction was not used because no appropriate method has been established for our SPECT system. Scatter correction was performed using the triple-energy window method. This method makes it possible to substantially reduce scatter activity between the left ventricular cavity and left ventricular myocardium and provides more accurate measurement of the input and output functions without contamination due to mutual activity (*9*). Moreover, the mean K values, including those for the superficial and deep segments of the left ventricle, were calculated in normal control subjects and DxMD patients. This averaging process tends to reduce the influence of tissue attenuation.

CONCLUSION

Analysis of BMIPP dynamic SPECT data by the Rutland method is useful for detecting qualitative differences in BMIPP metabolism in various types of myocardial damage. It is speculated that the fatty acid metabolic disorder is characterized by a delay in metabolism in DxMD and by increased backdiffusion in IHD. We are currently developing new software for creating functional images such as bull's-eye maps generated from the regional K values and the duration of the linear portion in the Rutland equation. Such software should make recognition and differentiation of fatty acid metabolic disorders an easy matter.

ACKNOWLEDGMENTS

The authors thank Shigeru Aoki and Shigeki Tsuboi for their cooperation and encouragement. An abstract of this study was presented at the 47th Annual Meeting of the Society of Nuclear Medicine, St. Louis, Missouri, June 3–7, 2000.

REFERENCES

1. Neely JR, Rovetto MJ, Oram JF. Myocardial utilization of carbohydrate and lipids. *Prog Cardiovasc Dis.* 1972;15:685–698.
2. Knapp FF, Ambrose KR, Goodman MM. New radioiodinated methyl-branched fatty acids for cardiac studies. *Eur J Nucl Med.* 1986;12(suppl):S39–S44.
3. Knapp FF, Kropp J, Goodman MM, et al. The development of iodine-123-methyl-branched fatty acids and their applications in nuclear cardiology. *Ann Nucl Med.* 1993;7:SII-1–SII-14.
4. Nakata T, Hashimoto A, Kobayashi H, et al. Outcome significance of thallium-201 and iodine-123 BMIPP perfusion-metabolism mismatch in preinfarction angina. *J Nucl Med.* 1998;39:1492–1499.
5. Hosokawa R, Nohara R, Fujibayashi Y, et al. Myocardial metabolism of ^{123}I-BMIPP in a canine model with ischemia: implications of perfusion-metabolism mismatch on SPECT images in patients with ischemic heart disease. *J Nucl Med.* 1999;40:471–478.
6. Hosokawa R, Nohara R, Okuda K, et al. Cardiac metabolism of I-123-β-methyl-ρ-iodophenyl pentadecanoic acid (I-123 BMIPP) in normal dogs and those pretreated with carnitine palmitoyltranseferase I inhibitor (etomoxir): contribution of α- and β-oxidation [abstract]. *J Nucl Med.* 1995;36(suppl):137P.
7. Fujibayashi Y, Yonekura Y, Takemura Y, et al. Myocardial accumulation of iodinated beta-methyl-branched fatty acid analogue, iodine-125-15-(p-iodophenyl)-3-(R,S)methylpentadecanoic acid (BMIPP), in relation to ATP concentration. *J Nucl Med.* 1990;31:1818–1822.
8. Saito K, Takeda K, Okamoto S, et al. Detection of doxorubicin cardiotoxicity by using iodine-123 BMIPP early dynamic SPECT: quantitative evaluation of early abnormality of fatty acid metabolism with the Rutland method. *J Nucl Cardiol.* 2000;7:553–561.
9. Ichihara T, Ogawa K, Motomura N, Kubo A, Hashimoto S. Compton scatter compensation using the triple-energy window method for single- and dual-isotope SPECT. *J Nucl Med.* 1993;34:2216–2221.
10. Rutland MD. A single injection technique for subtraction of blood background in ^{131}I-hippuran renograms. *Br J Radiol.* 1979;52:134–137.
11. Knapp FF. Myocardial metabolism of radioiodinated BMIPP. *J Nucl Med.* 1995;36:1051–1054.
12. Hwang EH, Taki J, Yasue S, et al. Absent myocardial iodine-123-BMIPP uptake and platelet/monocyte CD36 deficiency. *J Nucl Med.* 1998;39:1681–1684.
13. Yamamichi Y, Kusuoka H, Morishita K, et al. Metabolism of iodine-123-BMIPP in perfused rat hearts. *J Nucl Med.* 1995;36:1043–1050.
14. Fujibayashi Y, Nohara R, Hosokawa R, et al. Metabolism and kinetics of iodine-123-BMIPP in canine myocardium. *J Nucl Med.* 1996;37:757–761.
15. Morishita S, Kusuoka H, Yamamichi Y, et al. Kinetics of radioiodinated species in subcellular fractions from rat hearts following administration of iodine-123-labelled 15-(p-iodophenyl)-3(R,S)-methylpentadecanoic acid (^{123}I-BMIPP). *Eur J Nucl Med.* 1996;23:383–389.
16. Nohara R, Okuda K, Ogino M, et al. Evaluation of myocardial viability with iodine-123-BMIPP in a canine model. *J Nucl Med.* 1996;37:1403–1407.
17. Takeda K, Saito K, Makino K, et al. Iodine-123-BMIPP myocardial washout and cardiac work during exercise in normal and ischemic hearts. *J Nucl Med.* 1997;38:559–563.
18. Matsunari I, Saga T, Taki J, et al. Kinetics of iodine-123-BMIPP in patients with prior myocardial infarction: assessment with dynamic rest and stress thallium-201 SPECT. *J Nucl Med.* 1994;35:1279–1285.
19. Makino K, Okamoto R, Saito K, et al. Simple diagnostic procedure in patient with

ischemic heart disease: assessment with dynamic iodine-123 BMIPP SPECT compared with stress thallium-201 SPECT [abstract]. *J Nucl Med.* 1997; 38(suppl):165P–166P.
20. Kobayashi H, Kusakabe K, Momose M, et al. Evaluation of myocardial perfusion and fatty acid uptake using a single injection of iodine-123-BMIPP in patients with acute coronary syndromes. *J Nucl Med.* 1998;39:1117–1122.
21. Hosokawa R, Nohara R, Fujibayashi Y, et al. Myocardial kinetics of iodine-123-BMIPP in canine myocardium after regional ischemia and reperfusion: implications for clinical SPECT. *J Nucl Med.* 1997;38:1857–1863.
22. Olson RD, Mushlin PS, Brenner DE, et al. Doxorubicin cardiotoxicity may be caused by its metabolite, doxorubicinol. *Proc Natl Acad Sci USA.* 1988;85:3585–3589.
23. Billingham ME, Mason JW, Bristow MR, Daniels JR. Anthracycline cardiomyopathy monitored by morphologic changes. *Cancer Treat Rep.* 1978;62:865–872.
24. Goormaghtigh E, Pollakis G, Ruysschaert JM. Mitochondrial membrane modifications induced by adriamycin-mediated electron transport. *Biochem Pharmacol.* 1982;32:889–893.
25. Erland JFD, Poul KJ. Destruction of phospholipids and respiratory-chain activity in pig-heart submitochondrial particles induced by an adriamycin-iron complex. *Eur J Biochem.* 1983;132:551–556.
26. Seraydarian MW, Artaza L. Modification by adenosine of the effect of adriamycin on myocardial cells in culture. *Cancer Res.* 1979;39:2940–2944.
27. Neri B, Cini-Neri G, D'Alterio M. Effect of anthracyclines and ATP intracellular concentration in rat heart slices. *Biochem Biophys Res.* 1984;125:954–960.
28. Kataoka K, Nohara R, Hosokawa R, et al. Myocardial lipid metabolism in compensated and advanced stages of heart failure: evaluation by canine pacing model with BMIPP. *J Nucl Med.* 2001;42:124–129.